

Examining the Observability of Emergent Behavior as a Function of Reduced Model Order

Zhaohui Yang and Kshitij Jerath

Abstract— Current work on complex systems has been heavily focused on network interactions and network structure, without significant emphasis on the emergent phenomena that characterize such systems. In the included work, the ability to perceive or observe emergent behavior in complex systems has been studied. Specifically, by identifying emergent behavior as the dynamics of reduced-order models of the self-organizing systems, the observability of the emergent phenomena can be studied as a function of the model order. Included analytical results show the relationship between observability metrics of the full- and reduced-order models. Singular perturbation techniques have been used to perform model order reduction for nonlinear systems such as the Hyper Rössler and coupled Hindmarsh-Rose neuron models. Results indicate that accuracy increases and observability decreases with increasing model order. The trade-off between accuracy and observability metrics has been used to propose a predictive metric that identifies the desirable order at which to model emergent behavior.

I. INTRODUCTION

Emergent behavior refers to collective phenomenon observed in several large-scale systems, when examined from a global or macroscopic perspective [1]. Several natural and engineered systems, such as school of fish [2], neurons [3], traffic jams [4] etc., exhibit emergent behavior. Researchers have been fascinated with the idea of emergent behavior and self-organizing systems for several decades [5], but in recent times there has been a concerted scientific effort to impart additional mathematical rigor to these concepts [6][7]. There is increasing understanding in the research community that while self-organization refers to systems whose dynamics reside on a low-dimensional manifold and have an intrinsic structure or order [8], the term ‘emergent behavior’ should be reserved for situations where such self-organizing dynamics can actually be observed [9]. As such, the detection of emergent behavior is largely governed by (a) the order of the model being used to describe the self-organizing system dynamics, (b) the spatial scale of observation, and (c) structure of the observer. In this paper, we discuss the role of the first factor, i.e. the model order, on the observability of emergent behavior, with a discussion of other factors to follow in upcoming publications.

There is a critical need for this work that goes beyond the mere detection of emergence. Prediction and control of emergent behavior are open problems in the field of complex systems, with broad applications across diverse domains. For example, in the context of human neuronal systems, approximately 50 millions people are affected by epilepsy,

Both authors are affiliated to the School of Mechanical and Materials Engineering at the Washington State University, Pullman, WA, 99164, USA. e-mail: (zhaohui.yang@wsu.edu, kshitij.jerath@wsu.edu)

of which up to 40% may continue to have seizures despite optimal treatment [10]. The ability to identify and predict emergent seizure events holds the potential to impact a significant number of lives. One way to approach the problem is to create high-dimensional microscopic-scale models that attempt to capture the dynamics of every individual neuron, but this approach is computationally expensive [11]. Moreover, it is well-known that observing real-world large-scale complex systems (such a human brain) would require significant sensing equipment that makes the real-world implementation of such an approach intractable. On the other hand, in this paper we seek to identify the trends in accuracy and observability of emergent behavior (such as emergent seizure events) are known as a function of the system model order. With this knowledge, an appropriate model order can be chosen that ‘optimally’ describes the dynamics of the emergent behavior, which in turn can be leveraged for prediction and control. For the purpose of this paper, we use coupled singularly perturbed systems as prototypical examples of high-dimensional self-organizing systems that exhibit emergent behavior that resides on a low-dimensional manifold.

II. LITERATURE REVIEW

The study of observability and controllability can be traced back to the development of state-space models by Kalman [12]. While the state-space model was readily adapted to study observability of linear systems, its applicability to nonlinear systems was somewhat limited. Later works to extend the analysis of observability to nonlinear systems were performed by the likes of Hermann [13], Krener [14], Lobry [15], and Sussmann [16]. However, while these works were extremely useful, they could not be utilized to identify the ease of observing a nonlinear system, given a set of outputs. In other words, they failed to distinguish if one nonlinear system was more easily observed than another. Recent works by Letellier [17], have sought to overcome that limitation by developing metrics of observability that will be discussed in more detail in Section III. However, to the authors’ knowledge, neither of these works has been used to study the trends of observability as it relates to model order. In this work, we will utilize these measures of nonlinear observability to identify trends in observability of emergent behavior, which in turn may prove useful to identify an optimal model order to observe, predict, and control emergent behavior.

The second aspect of this study is to identify a model order reduction (MOR) technique to simplify the model used

to describe the self-organized system dynamics, which may eventually manifest as emergent behavior to the observer. Several MOR techniques have been developed over the past decades, the most commonly used among them being the balanced truncation. The fundamental principle that dictates the balanced truncation MOR technique is the removal of modes that are difficult to observe or control, and retaining only the observable and controllable modes of the system. However, we make no assumptions about the observability or controllability of the low-dimensional dynamics, since emergent behavior is not necessarily either controllable or observable. Another commonly-used MOR technique relies on Krylov subspaces, and builds upon the Arnoldi or Lanczos algorithm. The Krylov-subspace-based methods are computationally fast and highly parallelizable, and are widely used for order reduction of large, sparse linear systems. However, since the dynamics of a self-organized system reside on a low-dimensional manifold, we turn to singular perturbation methods to present this analysis. Singular perturbation methods are primarily used for model order reduction of systems with time-scale separation, i.e. in systems whose behavior is separated into slow and fast dynamics. The functional description of the dynamics is given by:

$$\begin{aligned}\dot{x} &= f(x, z, u) \\ \epsilon \dot{z} &= g(x, z, u)\end{aligned}\quad (1)$$

where $x \in \mathbb{R}^n$ represents the slow variables of the system, whose dynamics reside on a low-dimensional slow manifold, and $z \in \mathbb{R}^m$ represents the fast variables of the system, which evolve quickly towards the slow manifold, and ϵ is a small positive scalar that quantifies the time-scale separation. Upon performing the order reduction, the system model reduces to:

$$\dot{x} = f(x, z(x, u), u) \quad (2)$$

where the solution $z(x, u)$ of $g(x, z, u) = 0$, which defines the slow manifold of the self-organizing system, can be substituted into the slow dynamics to obtain the reduced order model. This MOR approach is only applicable for systems where time-scale separation is evident. While many self-organizing systems do not clearly exhibit such time-scale separation (e.g. self-organized traffic jams [4]), the use of the singularly perturbed systems as a prototypical example is justified to establish the trends in observability as a function of reduced model order. Moreover, such time-scale separation is evident in other self-organizing systems, as discussed in the observability study of the coupled multiple-neuron model in Section V.

III. MEASURE OF OBSERVABILITY FOR NONLINEAR SYSTEMS

The key issue for analyzing and predicting emergent behavior in complex self-organizing systems is to gauge how ‘far’ the system is from being unobservable [18]. The observability of self-organizing systems, and nonlinear systems in general, varies with time along its trajectory in state-space. To assess the observability of such nonlinear systems, we evaluate the Lie derivative and an associated

observability metric at every time instant along the system’s trajectory. The Lie derivative for the i th component of the vector field $f(\mathbf{x})$ is defined as:

$$\mathcal{L}_{f_i}(\mathbf{x}) := \sum_{k=1}^m \frac{\partial f_i(\mathbf{x})}{\partial x_k} f_k \quad (3)$$

and the higher order Lie derivatives may be evaluated recursively using the lower-order Lie derivatives as follows:

$$\mathcal{L}_{f_i}^n(\mathbf{x}) := \mathcal{L}_{f_i}(\mathcal{L}_{f_i}^{n-1}(\mathbf{x})) \quad (4)$$

The observability grammian is given by the observability matrix \mathcal{Q} as follows:

$$\mathcal{Q} := \left[\frac{\partial \mathcal{L}_f^0[h(\mathbf{x})]}{\partial \mathbf{x}}, \frac{\partial \mathcal{L}_f^1[h(\mathbf{x})]}{\partial \mathbf{x}}, \dots, \frac{\partial \mathcal{L}_f^{n-1}[h(\mathbf{x})]}{\partial \mathbf{x}} \right]^T \quad (5)$$

where $h(\mathbf{x})$ represents the output of the system. The observability matrix \mathcal{Q} can be determined for both full- and reduced-order systems. A comparison of their functional forms not only helps assess how much observability is ‘retained’ after order reduction, but also assess which observer structure helps retain it the most (See Section IV).

A. Observability Metric

Complex systems may be observable in certain sections of their state trajectories, and unobservable in other sections. To assess their observability, a metric for nonlinear systems can be defined using the observability matrix \mathcal{Q} , similar to observability metrics such as minimum singular values for linear systems. Building on the works of Aguirre and Letellier [17], an observability metric known as the degree of observability can be defined as:

$$\delta(\mathbf{x}, t) = \frac{|\lambda_{\min}[\mathcal{Q}^T \mathcal{Q}, \mathbf{x}(t)]|}{|\lambda_{\max}[\mathcal{Q}^T \mathcal{Q}, \mathbf{x}(t)]|} \quad (6)$$

where $\lambda_{\max}[\mathcal{Q}^T \mathcal{Q}, \mathbf{x}(t)]$ indicates the maximum eigenvalue of matrix $\mathcal{Q}^T \mathcal{Q}$ at a specific location in the system trajectory, and $\mathbf{x}(t)$ denotes the observed variable at time t . The values of the observability metric vary in the interval $[0, 1]$, with a larger value indicating better observability. This metric may be used to study the reduced-order model of the complex system, as well as determine spatial locations within the state space where the complex system has high (or low) tendency towards being observable.

B. Relationship between Full- and Reduced-order Metrics

We assume that \mathcal{Q}_o is a multidimensional observability matrix for the full-order system, and \mathcal{Q}_{11} is its block component and represents the observability matrix of the reduced-order system:

$$\mathcal{Q}_o = \begin{bmatrix} \mathcal{Q}_{11} & \mathcal{Q}_{12} \\ \mathcal{Q}_{21} & \mathcal{Q}_{22} \end{bmatrix} \quad (7)$$

For the full-order system, the observability matrix can be evaluated using the matrix $\mathcal{K}_o = \mathcal{Q}_o^T \mathcal{Q}_o$, given by:

$$\mathcal{K}_o = \begin{bmatrix} \mathcal{Q}_{11} \mathcal{Q}_{11}^T + \mathcal{Q}_{12} \mathcal{Q}_{12}^T & \mathcal{Q}_{11} \mathcal{Q}_{21}^T + \mathcal{Q}_{12} \mathcal{Q}_{22}^T \\ \mathcal{Q}_{21} \mathcal{Q}_{11}^T + \mathcal{Q}_{22} \mathcal{Q}_{12}^T & \mathcal{Q}_{21} \mathcal{Q}_{21}^T + \mathcal{Q}_{22} \mathcal{Q}_{22}^T \end{bmatrix} \quad (8)$$

We now examine the differences in full- and reduced-order observability, by focusing our attention on the sub-matrix \mathcal{K}_s of the matrix \mathcal{K}_o corresponding to the full-order observability metric, as well as \mathcal{K}_r , which will be used to evaluate the reduced-order observability metric:

$$\mathcal{K}_s = [\mathcal{Q}_{11} \mathcal{Q}_{11}^T + \mathcal{Q}_{12} \mathcal{Q}_{12}^T], \quad \mathcal{K}_r = [\mathcal{Q}_{11} \mathcal{Q}_{11}^T] \quad (9)$$

From Cauchy's interlace theorem [19], the relation between eigenvalues of symmetric matrices (such as \mathcal{K}_o) before and after removing certain pair of columns and rows are:

$$\lambda_{min}^o \leq \lambda_{min}^s, \quad \lambda_{max}^o \geq \lambda_{max}^s \quad (10)$$

In addition, under the condition that eigenvalues of $\mathcal{Q}_{12} \mathcal{Q}_{12}^T$ tend to zero, the following relationship for the eigenvalue ratios can be obtained:

$$\frac{\lambda_{min}^r}{\lambda_{max}^r} \approx \frac{\lambda_{min}^s}{\lambda_{max}^s} \quad (11)$$

Combining (10) and (11) leads to the conclusion that:

$$\frac{\lambda_{min}^r}{\lambda_{max}^r} \approx \frac{\lambda_{min}^s}{\lambda_{max}^s} \geq \frac{\lambda_{min}^o}{\lambda_{max}^o} \quad (12)$$

Thus if observability matrix of reduced order system is a block component of full order system, then we could predict that the reduced order system is more observable than full order system:

$$\delta_r(x, t) \geq \delta_o(x, t) \quad (13)$$

IV. OBSERVABILITY VARIATION AS A FUNCTION OF MODEL ORDER

In this section, we will present an analytical comparison of the observability metrics of full- and reduced-order models, using the hyperchaotic Rössler system as an example. The analysis will also help guide the choice of observable for examining emergent behavior. We begin with the general singularly perturbed system described in (1), which may be re-written as follows:

$$\dot{\mathbf{x}} = \begin{bmatrix} \dot{x} \\ \dot{z} \end{bmatrix} = \begin{bmatrix} f(x, z) \\ g(x, z)/\epsilon \end{bmatrix} \quad (14)$$

and for which the output is given by $y = h(\mathbf{x})$. The i^{th} row of the associated observability matrix for the full-order system \mathcal{Q}_0 may be assumed to consist of two components:

$$\mathcal{Q}_o^i = \frac{\partial \mathcal{L}_f^i[h(\mathbf{x})]}{\partial \mathbf{x}} = [\mathcal{Q}_s^i \mid \mathcal{Q}_f^i]$$

where \mathcal{Q}_s^i indicates the partial derivative with respect to the slow variables (x), and \mathcal{Q}_f^i indicates partial derivative with respect to the fast variables (z). Additionally, we distinguish between the full-order and the reduced-order observability matrices (\mathcal{Q}_0 and \mathcal{Q}_r , respectively) using the following notation:

$$\mathcal{Q}_o = \left[\begin{array}{c|c} \mathcal{Q}_s^0 & \mathcal{Q}_f^0 \\ \mathcal{Q}_s^1 & \mathcal{Q}_f^1 \\ \vdots & \vdots \\ \hline \vdots & \vdots \\ \mathcal{Q}_s^{n+m-1} & \mathcal{Q}_f^{n+m-1} \end{array} \right] \quad \text{and} \quad \mathcal{Q}_r = \left[\begin{array}{c} \mathcal{Q}_r^0 \\ \mathcal{Q}_r^1 \\ \vdots \\ \mathcal{Q}_r^{n-1} \end{array} \right] \quad (15)$$

By comparing the observability matrices \mathcal{Q}_0 and \mathcal{Q}_r , we show that the observability matrix for the reduced-order system is a block component of the full-order observability matrix as follows:

$$\mathcal{Q}_o = \left[\begin{array}{c|c} \mathcal{Q}_r & \cdots \\ \hline \cdots & \cdots \end{array} \right] \quad (16)$$

Consequently, the **key insight** of this work is to realize that eigenvalues of $\mathcal{Q}_r^T \mathcal{Q}_r$ necessarily lie between the minimum and maximum eigenvalues of $\mathcal{Q}_o^T \mathcal{Q}_o$, resulting in the observability metric of the reduced-order system being higher than that of the full-order singularly perturbed system.

A. Analytical Comparison of Full- and Reduced-order Observability Matrices

In this analysis, we assume that the system output is scalar and a linear function of the slow variables, i.e. $y = h(\mathbf{x}) = h(x)$. Then, the slow dynamics component in the first row of full-order observability matrix is given by:

$$\mathcal{Q}_0^1 = \frac{\partial \mathcal{L}_f^0[h(\mathbf{x})]}{\partial \mathbf{x}} = \frac{\partial \mathcal{L}_f^0[h(x)]}{\partial x} = \frac{\partial h(x)}{\partial x} = C \quad (17)$$

The subsequent rows can be generated using the recursive relationship of Lie derivatives, so that entries for the 2nd row of full- and reduced-order models are $[C \frac{\partial f}{\partial x} \mid C \frac{\partial f}{\partial z}]$ and $C \frac{\partial f}{\partial x}$, respectively. The key difference between these entries corresponding to slow dynamics in the 3rd row lies in terms $\frac{\partial f}{\partial z} \frac{\partial g}{\partial x}$ and $\frac{\partial f}{\partial x} \frac{\partial f}{\partial z} \frac{\partial z}{\partial x}$.

Similarly, we can examine the difference between the i^{th} rows of the observability matrices \mathcal{Q}_0^i and \mathcal{Q}_r^i . The i^{th} row of the full-order observability matrix is given by:

$$\begin{aligned} \mathcal{Q}_0^i &= [\mathcal{Q}_s^i(x, z), \mathcal{Q}_f^i(x, z)] \\ &= \left[\begin{array}{c} \frac{\partial \mathcal{Q}_s^{i-1}}{\partial x} f + \frac{\partial f}{\partial x} \mathcal{Q}_s^{i-1} + \frac{\partial \mathcal{Q}_f^{i-1}}{\partial x} \frac{g}{\epsilon} + \frac{\partial g}{\epsilon \partial x} \mathcal{Q}_f^{i-1}, \\ \frac{\partial \mathcal{Q}_s^{i-1}}{\partial z} f + \frac{\partial f}{\partial z} \mathcal{Q}_s^{i-1} + \frac{\partial \mathcal{Q}_f^{i-1}}{\partial z} \frac{g}{\epsilon} + \frac{\partial g}{\epsilon \partial z} \mathcal{Q}_f^{i-1} \end{array} \right] \end{aligned} \quad (18)$$

where the components corresponding to the slow and fast dynamics (\mathcal{Q}_s^i and \mathcal{Q}_f^i , respectively) have been shown separated by commas. The corresponding i^{th} row of the reduced-order observability matrix is given by:

$$\begin{aligned} \mathcal{Q}_r^i(x, z) &= \\ &= \left[\begin{array}{c} \frac{\partial \mathcal{Q}_r^{i-1}}{\partial x} f + \frac{\partial f}{\partial x} \mathcal{Q}_r^{i-1} + \frac{\partial \mathcal{Q}_r^{i-1}}{\partial z} \frac{\partial z}{\partial x} f + \frac{\partial f}{\partial z} \frac{\partial z}{\partial x} \mathcal{Q}_r^{i-1} \end{array} \right] \end{aligned} \quad (19)$$

Additionally, \mathcal{Q}_s^{i-1} and \mathcal{Q}_f^{i-1} are both obtained from the previous row of the observability matrix. Rewriting $\mathcal{L}_f^{i-2}[h(x)]$ as $F(\mathcal{Q}_s^{i-2}, \mathcal{Q}_f^{i-2})$, using recursive property of Lie derivative, and evaluating the appropriate Jacobian, we obtain a simplified expression for the components of the observability matrix:

$$\mathcal{Q}_s^{i-1} = \frac{\partial F(\mathcal{Q}_s^{i-2}, \mathcal{Q}_f^{i-2})}{\partial x}, \quad \mathcal{Q}_f^{i-1} = \frac{\partial F(\mathcal{Q}_s^{i-2}, \mathcal{Q}_f^{i-2})}{\partial z} \quad (20)$$

Now, we can infer the following using (20):

$$\begin{aligned} \frac{\partial \mathcal{Q}_f^{i-1}}{\partial x} &= \frac{\partial F(\mathcal{Q}_s^{i-2}, \mathcal{Q}_f^{i-2})}{\partial z \partial x}, \quad \frac{\partial \mathcal{Q}_s^{i-1}}{\partial z} = \frac{\partial F(\mathcal{Q}_s^{i-2}, \mathcal{Q}_f^{i-2})}{\partial z \partial x} \\ \Rightarrow \frac{\partial \mathcal{Q}_f^{i-1}}{\partial x} &= \frac{\partial \mathcal{Q}_s^{i-1}}{\partial z} = \frac{\partial \mathcal{Q}_r^{i-1}}{\partial z} \end{aligned} \quad (21)$$

In addition, if the fourth components of the i^{th} row of the full- and reduced-order observability matrices are also identical, then the matrix \mathcal{Q}_r is indeed a block component of \mathcal{Q}_o . Then, as a consequence of the interlacing theorem of symmetric matrices [19], the eigenvalues of $\mathcal{Q}_r^T \mathcal{Q}_r$ will necessarily lie between the minimum and maximum eigenvalues of $\mathcal{Q}_o^T \mathcal{Q}_o$, indicating that the reduced-order observability is better than full-order observability.

B. Hyper-chaotic Rössler system

The hyper-chaotic Rössler system is used to illustrate the effect of choice of output on system observability:

$$\begin{aligned} \dot{x} &= -y - z \\ \dot{y} &= x + ay + w \\ \dot{z} &= b + xz \\ \dot{w} &= -cz + dw \end{aligned} \quad (22)$$

where x , y , z , and w are all scalars, and a , b , c , and d represent scalar model parameters. With the appropriate choice of parameters, the variable w can be made to possess fast dynamics, so that the system dynamics are time-scale separated and singular perturbation methods can be used to reduce the model order. If w has fast dynamics, then $-cz + dw \rightarrow 0$. In this situation, the slow manifold is given by $dw = cz$ or instead, $w = kz$, where $k = c/d$. As a result, the hyper-chaotic Rössler system reduces to:

$$\begin{aligned} \dot{x} &= -y - z \\ \dot{y} &= x + ay + kz \\ \dot{z} &= b + xz \end{aligned} \quad (23)$$

From analytical consideration presented in (21), all but the fourth terms of the observability matrices of the full- and reduced-order Rössler systems are identical. Comparing the fourth terms of \mathcal{Q}_o^i and \mathcal{Q}_r^i (defined in (18) and (19)) for the current example, we observe:

$$\text{From } \mathcal{Q}_o^i : C \frac{\partial f}{\partial z} \frac{\partial g}{\partial x} = C \begin{bmatrix} 0 & 0 & 0 \\ 0 & 0 & -c \\ 0 & 0 & 0 \end{bmatrix} \quad (24)$$

$$\text{From } \mathcal{Q}_r^i : C \frac{\partial f}{\partial x} \frac{\partial f}{\partial z} \frac{\partial z}{\partial x} = C \begin{bmatrix} 0 & 0 & -c \\ 0 & 0 & -ac \\ 0 & 0 & 0 \end{bmatrix} \quad (25)$$

Clearly, if the scalar linear output is $h(\mathbf{x}) = z$, i.e. the third state, so $C = [0, 0, 1]$, then the terms in the above two equations are identical (and equal to zero). As a consequence, \mathcal{Q}_r would be a block component of the \mathcal{Q}_o and the Rössler system would have better observability than the hyper-chaotic Rössler system with the state variable z as the output. If any other state variable is chosen as the output,

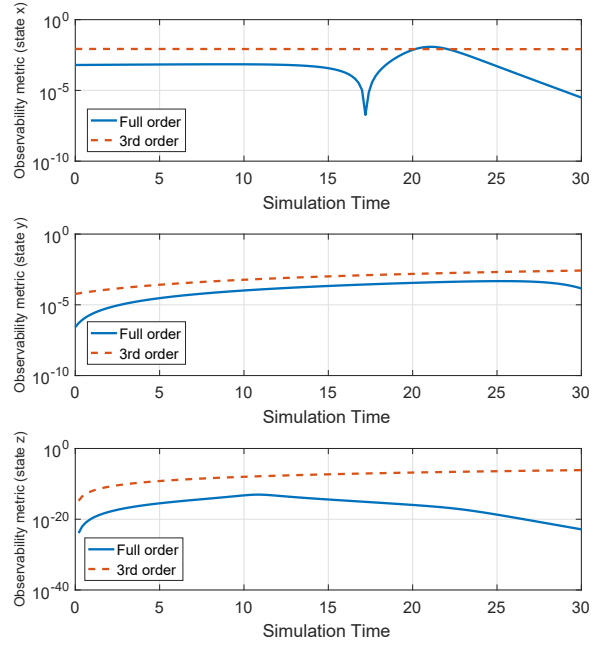


Fig. 1. Comparisons of the observability metrics of full- and reduced-order system for different outputs under step input. Notice the difference in the y-axis scales for state z as compared to the other state variables.

then the fourth terms will be different, and we will not be able to make a similar claim about the observability of the reduced order system. Indeed, as shown in Fig. 1, choosing z as the output variable results in significant improvement in observability as compared to other choices of variables.

V. THE ACCURACY VS. OBSERVABILITY TRADE-OFF: MULTI-NEURON EXAMPLE

Models of neuronal bursting have been studied extensively, and the emergent behavior of a neural system is difficult to predict by examining a single neuron in isolation. In this section, we examine the singularly perturbed coupled Hindmarsh-Rose model of bursting neurons and assess the observability and accuracy as a function of reduced model orders [20].

A. Coupled Hindmarsh-Rose Neuron Model

Certain neurons in the brain, especially during periods of drowsiness, inattentiveness, or sleep exhibit spike-burst activity. This behavior can be modeled at the neuron level using time-scale separation for the coupled Hindmarsh-Rose model as shown below:

$$\begin{aligned} \dot{x}_1 &= y_1 - ax_1^3 + bx_1^2 - z_1 + \epsilon(x_1 - x_2) \\ \dot{y}_1 &= c - dx_1^2 - y_1 \\ \dot{z}_1 &= r[(x_1 - x_0) - z_1] \\ \dot{x}_2 &= y_2 - ax_2^3 + bx_2^2 - z_2 + \epsilon(x_2 - x_1) \\ \dot{y}_2 &= c - dx_2^2 - y_2 \\ \dot{z}_2 &= r[(x_2 - x_0) - z_2] \end{aligned} \quad (26)$$

where x is the membrane potential, y is associated with the fast current, Na^+ or K^+ , z with the slow current, and the model parameters are given by $a = 1.0, b = 3.0, c = 1.0, d = 5.0, s = 4.0, r = 0.006, x_0 = -1.60$. The fast variables are given by x and y , whereas z denotes the slow variable. Here r represents the ratio of fast/slow times scales.

After reducing the model order of this coupled singularly perturbed system (by setting the dynamics of the fast variables to zero), and rescaling the time to align with the slower dynamics $\tau = rt$ (where r plays the role of ϵ), the reduced order dynamics are given by:

$$\begin{aligned}\dot{z}_1 &= (x_1 - x_0) - z_1 \\ \dot{z}_2 &= (x_2 - x_0) - z_2\end{aligned}\quad (27)$$

where slow manifold can be modified to read as $x_1 = g_1(z_1, x_2)$ and $x_2 = g_2(z_2, x_1)$. Now it is often intractable to obtain the exact solution for the slow manifold, so the system simulation can instead be carried out using the quasi-steady-state model by evaluating:

$$\dot{x}_1 = \frac{\partial g_1}{\partial z_1} \dot{z}_1 + \frac{\partial g_1}{\partial x_2} \dot{x}_2, \quad \dot{x}_2 = \frac{\partial g_2}{\partial z_2} \dot{z}_2 + \frac{\partial g_2}{\partial x_1} \dot{x}_1 \quad (28)$$

and substituting the appropriate values of x_1 and x_2 into the reduced model (27). Fig. 2 provides a comparison of the full- and reduced-order models for a single neuron observability. It is evident that the reduced order model has better observability than the full-order model for significant periods of time.

B. Coupled Multiple-neuron System with Three Neurons

In this subsection, we examine the observability and accuracy trends as we reduce the model order for a coupled Hindmarsh-Rose model with three neurons arranged in a linear topology. The model is given by:

$$\begin{aligned}\dot{z}_i &= \frac{1}{r_i} \left\{ y_i - ax_i^3 + bx_i^2 - z_i + I_{ext} + \epsilon \sum_j G_{ij} H(\mathbf{x}_j) \right\} \\ \dot{y}_i &= \frac{1}{r_i} (c - dx_i^2 - y_i) \\ \dot{z}_i &= (x_i - x_0) - z_i\end{aligned}\quad (29)$$

where r_i denotes the ratio for the fast/slow time scales for each neuron and G_{ij} is the adjacency matrix related to the coupling among neurons. The values for r_i in different neurons are set to 0.001, 0.02, 0.1, and other parameters remain unchanged. Order reduction was conducted based on the time scales, with the fastest time scales removed first, until only the slow states z_1, z_2 and z_3 are left.

Now, a dynamical model for a self-organizing must not only possess good observability, it should also accurately represent the real-world emergent behavior. This emphasis on accurate representation of the system dynamics is especially true for reduced-order models. As the ratio over fast/slow time scale starts decrease, we could do order reduction sequentially by using singular perturbation. Thus, a trade-off exists between our ability to observe the reduced-order

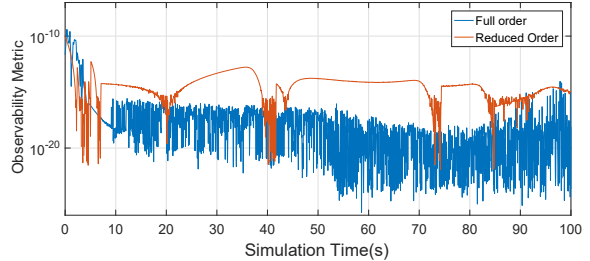


Fig. 2. Comparisons of the observability for full- and reduced-order systems towards step input on the state z . The reduced-order system is more observable than the full-order system.

model, and the ability of the reduce-order model to mimic the real-world dynamics (or full-order model). In order to examine this trade-off for the coupled Hindmarsh-Rose neuron models, we propose two normalized metrics – one for the observability and another for the accuracy of the reduced-order model. The normalized metric for observability is:

$$\Delta(i) = \left| \frac{\delta_i(x) - \delta_{min}(x)}{\delta_{max}(x) - \delta_{min}(x)} \right| \quad (30)$$

where $\Delta(\cdot)$ represents the normalized observability metric for reduced order model of order i , $\delta_i(x)$ denotes the observability metric defined in (6) for the reduced order model of order i , $\delta_{min}(x)$ denotes the observability metric for the reduced order model with minimum dimension, and $\delta_{max}(x)$ denotes the observability metric for the full order model. For example, for the 3 coupled neuron system, reduced iteratively through orders 9, 7, 5, and 3, the normalized observability metric may be written as:

$$\Delta(i) = \left| \frac{\delta_i(x) - \delta_3(x)}{\delta_9(x) - \delta_3(x)} \right| \quad (31)$$

Similarly the normalized accuracy metric \mathcal{A}_i for reduced order model of order i can be evaluated as:

$$\mathcal{A}(i) = \left| \frac{e_i - e_{min}}{e_{max} - e_{min}} \right| \quad (32)$$

where e_i is the L_1 norm of the error in output signal between the reduced order and full order model over a given time interval. Clearly, this normalized accuracy metric is only valid till dimension one less than the full-order dimension, since e_{max} evaluates the L_1 error norm of output between the maximum reduced order model and full order model. These metrics are evaluated for behaviors of the coupled neuron systems respectively at order 3, 5, 7, 9, and are included in Fig. 3. Moreover, it is evident from the structure that the normalized accuracy metric \mathcal{A}_i for lower order reduced models is lower than reduced-order models of higher order, since accuracy decreases with reducing order. On the other hand, the observability increases with reducing model order.

It is evident that accuracy decreases and observability increases with decreasing model order. Clearly there exists a trade-off between these two quantities. The trade-off can be

leverage to determine an ‘optimal’ predictive metric that can be used to best model emergent behavior in complex self-organizing systems. In this paper, we propose a predictive metric for emergent behavior that relies on the normalized observability and normalized accuracy to identify the model order that best captures the emergent behavior of a complex system, and is given by:

$$\mathcal{K}(i) = \left| \frac{\mathcal{A}(i) \cdot \Delta(i)}{\max|\mathcal{A}(i) \cdot \Delta(i)|} \right| \quad (33)$$

The authors do not claim the optimality of this metric in the sense proposed by Shalizi in [21]. Additionally, while we do not make a claim regarding the optimal order to use for modeling emergent behavior based on these results, this remains an interesting question to pursue further.

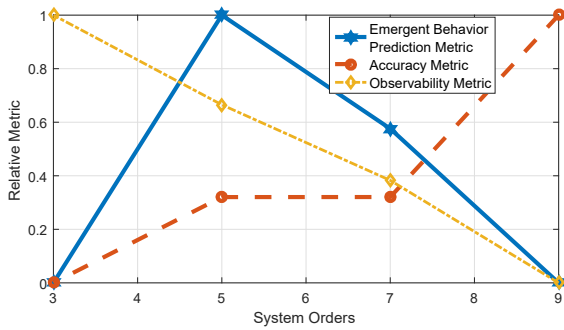


Fig. 3. Trends in accuracy and observability of emergent behavior as a function of the reduced model order. Also shown is the predictive metric for emergent behavior that holds the potential to identify the model order that is best suited to describe such behavior.

VI. CONCLUDING REMARKS AND FUTURE WORK

Emergent behavior is exhibited by several naturally occurring and engineered complex systems. Such behavior usually manifests in low-dimensional state space compared to the high-dimensional state space of the complex system. In this work, emergent behavior was represented by reduced order models of higher dimensional systems. The order reduction was carried out using singular perturbation methods for a hyper Rössler system and coupled Hindmarsh-Rose multiple-neuron model. Observability metrics for these nonlinear systems indicated that the reduced order models (emergent behaviors of the complex system) were more observable than the full-order models representative of complex systems. Moreover, there is evidence of a trade-off between the observability and accuracy of the emergent behavior at reduced orders, indicating that there may be an optimal modeling order that best captures the dynamics of a self-organizing system, while ensuring good observability.

This work has the potential to guide the design of observers for complex systems exhibiting emergent behavior. Moreover, once the observability (or the degree of observability) for a complex system and its accompanying emergent behavior can be established, this information may be used to design controllers to guide the complex system towards

desirable emergence and away from undesirable emergent behavior, such as self-organized traffic jams and cascading blackouts in power grids.

ACKNOWLEDGEMENTS

This work was partially supported by the National Science Foundation CMMI DCSD program (award no. 1663652).

REFERENCES

- [1] Z. Li, C. H. Sim, and M. Y. H. Low, “A survey of emergent behavior and its impacts in agent-based systems,” in *Industrial Informatics, 2006 IEEE International Conference on*. IEEE, 2006, pp. 1295–1300.
- [2] K. Tunstrøm, Y. Katz, C. C. Ioannou, C. Huepe, M. J. Lutz, and I. D. Couzin, “Collective states, multistability and transitional behavior in schooling fish,” *PLoS computational biology*, vol. 9, no. 2, p. e1002915, 2013.
- [3] J. A. Bonachela, S. De Franciscis, J. J. Torres, and M. A. Munoz, “Self-organization without conservation: are neuronal avalanches generically critical?” *Journal of Statistical Mechanics: Theory and Experiment*, vol. 2010, no. 02, p. P02015, 2010.
- [4] K. Jerath and S. N. Brennan, “Analytical prediction of self-organized traffic jams as a function of increasing acc penetration,” *IEEE Transactions on Intelligent Transportation Systems*, vol. 13, no. 4, pp. 1782–1791, 2012.
- [5] W. R. Ashby, “An introduction to cybernetics,” *The journal of general psychology*, 1957.
- [6] K. Jerath and S. Brennan, “Identification of locally influential agents in self-organizing multi-agent systems,” in *2015 American Control Conference (ACC)*. IEEE, 2015, pp. 335–340.
- [7] A. J. Roberts, *Model emergent dynamics in complex systems*. SIAM, 2014.
- [8] J.-M. Ginoux and B. Rosseto, “Invariant manifolds of complex systems,” in *Complex Systems and Self-organization Modelling*. Springer, 2009, pp. 41–49.
- [9] D. Polani, *Advances in Applied Self-organizing Systems*. Springer London, 2007, ch. Foundations and Formalizations of Self-organization, pp. 19–37.
- [10] S. Sinha and K. A. Siddiqui, “Definition of intractable epilepsy,” *Neurosciences (Riyadh)*, vol. 16, no. 1, pp. 3–9, 2011.
- [11] H. Markram, “The blue brain project,” *Nature Reviews Neuroscience*, vol. 7, no. 2, pp. 153–160, 2006.
- [12] R. E. Kalman, *New methods and results in linear prediction and filtering theory*. Research Institute for Advanced Studies, 1961.
- [13] R. Hermann and A. J. Krener, “Nonlinear controllability and observability,” *IEEE Transactions on automatic control*, vol. 22, no. 5, pp. 728–740, 1977.
- [14] A. J. Krener and A. Isidori, “Linearization by output injection and nonlinear observers,” *Systems & Control Letters*, vol. 3, no. 1, pp. 47–52, 1983.
- [15] C. Lobry, “Controllability of nonlinear systems on compact manifolds,” *SIAM Journal on Control*, vol. 12, no. 1, pp. 1–4, 1974.
- [16] H. J. Sussmann, “Existence and uniqueness of minimal realizations of nonlinear systems,” *Mathematical Systems Theory*, vol. 10, no. 1, pp. 263–284, 1976.
- [17] C. Letellier, L. Aguirre, and J. Maquet, “How the choice of the observable may influence the analysis of nonlinear dynamical systems,” *Communications in Nonlinear Science and Numerical Simulation*, vol. 11, no. 5, pp. 555–576, 2006.
- [18] A. J. Krener and K. Ide, “Measures of unobservability,” in *Decision and Control, 2009 held jointly with the 2009 28th Chinese Control Conference. CDC/CCC 2009. Proceedings of the 48th IEEE Conference on*. IEEE, 2009, pp. 6401–6406.
- [19] S. Fisk, “A very short proof of cauchy’s interlace theorem for eigenvalues of hermitian matrices,” *Am. Math. Mon.*, vol. 112, no. math. CA/0502408, p. 118, 2005.
- [20] J. L. Hindmarsh and R. Rose, “A model of neuronal bursting using three coupled first order differential equations,” *Proceedings of the royal society of London B: biological sciences*, vol. 221, no. 1222, pp. 87–102, 1984.
- [21] C. R. Shalizi, K. L. Shalizi, and R. Haslinger, “Quantifying self-organization with optimal predictors,” *Physical review letters*, vol. 93, no. 11, p. 118701, 2004.